


Exploring unconventional quantum criticality in the p -wave-paired Aubry-André-Harper modelTing Lv,^{1,2} Yu-Bin Liu,^{1,2} Tian-Cheng Yi,³ Liangsheng Li,⁴ Maoxin Liu,⁵ and Wen-Long You^{1,2,*}¹College of Physics, Nanjing University of Aeronautics and Astronautics, Nanjing 211106, China²Key Laboratory of Aerospace Information Materials and Physics (NUAA), MIIT, Nanjing 211106, China³Beijing Computational Science Research Center, Beijing 100193, China⁴Science and Technology on Electromagnetic Scattering Laboratory, Beijing 100854, China⁵School of Science, Beijing University of Posts and Telecommunications, Beijing 100876, China (Received 16 May 2022; revised 11 September 2022; accepted 7 October 2022; published 18 October 2022)

We have investigated scaling properties near the quantum critical point between the extended phase and the critical phase in the Aubry-André-Harper model with p -wave pairing, which have rarely been exploited as most investigations focus on the localization transition from the critical phase to the localized phase. We find that the spectrum-averaged entanglement entropy and the generalized fidelity susceptibility act as eminent universal order parameters of the corresponding critical point without gap closing. We introduce a Widom scaling *Ansatz* for these criticality probes to develop a unified theory of critical exponents and scaling functions. We thus extract the correlation-length critical exponent ν and the dynamical exponent z through the finite-size scaling given the system size increase in the Fibonacci sequence. The retrieved values of $\nu \simeq 1.000$ and $z \simeq 3.610$ indicate that the transition from the extended phase to the critical phase belongs to a different universality class from the localization transition. Our approach sets the stage for exploring the unconventional quantum criticality and the associated universal information of quasiperiodic systems in state-of-the-art quantum simulation experiments.

DOI: [10.1103/PhysRevB.106.144205](https://doi.org/10.1103/PhysRevB.106.144205)**I. INTRODUCTION**

The concept of disorder-induced localizations was originally addressed in the seminal work of Anderson [1] and still fuels a variety of new ideas and research directions. Notably, engineering random disorder remains an experimental challenge, and the theoretical study of randomly disordered system suffers from the necessity of disorder averaging. It is largely recognized that there is another class of systems in which the distribution of the disordered potential is not random, but showcases some quasiperiodic structures. Quasiperiodic disorder provides a midway between randomly disordered and clean systems for exploring novel phases of matter. The physics of quasiperiodic systems is known to show unconventional phenomena including mobility edges [2–5], fractal bands [6,7], many-body localization [8–11], topological features [12–14], and exotic forms of phases [15,16], as well as currently intensively investigated non-Hermiticities [17]. Remarkably, quasiperiodic systems have been observed in a number of systems, such as photonic crystals [18,19], cavity polaritons [20], cold atoms in bichromatic laser potentials [21–24], twisted bilayer graphene [25], and optical waveguides [26]. The continuing development of experimental techniques has led to a deeper understanding of quasiperiodic criticality [27–30] and associated universal information [31–34].

Among a diversity of quasiperiodic models, the Aubry-André-Harper (AAH) model [35–37] and its generalizations

are nowadays drawing increasing attention. The standard AAH model can be formally derived from a tight-binding square-lattice Hamiltonian in the presence of a magnetic field yielding the famous Hofstadter butterfly to a one-dimensional (1D) chain when the hopping amplitudes are the same [38]. A dual transformation between the coordinate and momentum spaces will yield the same Hamiltonian with hopping and potential amplitudes interchanged. As a consequence of the inherent self-duality, all the eigenstates of the system undergo Anderson localization transition from an extended phase (EP) to a localized phase (LP) at a critical value of the incommensurate potential strength [39,40], as was first shown by Aubry and André [41]. By contrast, all single-particle states localize for arbitrarily weak disorder in 1D systems with uncorrelated disorder [1]. During the past few years, a growing effort has been made to explore the effect of the self-duality breaking interactions to the AAH Hamiltonian. A peculiar direction is the inclusion of the p -wave superconducting pairing [42–44]. The reentrant localization transition can be established by analyzing inverse participation ratios (IPRs) of eigenspectra, the bandwidth distribution, and the level spacing distribution. The p -wave pairing term breaks the self-dual symmetry and splits the single transition into a three-phase spectral diagram. A critical phase (CP) crops up between the extended and localized phases [45–47]. The emerging CP exhibits various interesting features, such as power-law localization [48], critical spectral statistics [49–51], and multifractal behavior of wave functions [52,53]. In particular, the intermediate CP proliferates in the quantum magnetism described by the anisotropic XY chain under an irrationally modulated transverse field, which is

*wlyou@nuaa.edu.cn

equivalent to the AAH model with p -wave pairing through the celebrated Jordan-Wigner transformation [54–57]. The CP can be possibly detected by measuring the mean square displacement of the wave packet after a fixed time of expansion in the real space or the momentum distributions [58].

While most investigations focus on the phase transition between the CP and the LP, little is known about critical properties of the transition from the EP to the CP. The critical-localized phase transition is deemed as the reminiscence of Anderson localization transition in the absence of p -wave pairing, which coincides with a second-order transition from a topological superconducting phase to a topologically trivial localized phase [43]. The quench dynamics from the LP to the CP through the Kibble-Zurek mechanism and the gap scaling unveil the correlation-length exponent $\nu \simeq 1.000$ and the dynamical critical exponent $z \simeq 1.373$ [47], which are consistent with numerical results of the generalized fidelity susceptibility (GFS) $\nu \simeq 1.000$, $z \simeq 1.388$ [59]. However, the gap scaling fails owing to the apparent nonclosure of the spectral gap across the extended-critical transition with periodic boundary conditions, which is beyond the regime of thermodynamic phase transition. Therefore, there is a clear need to identify observables for the characterization of the EP-CP transition that can be measured in state-of-the-art quantum simulators and are easy to compute numerically as well.

Motivated by these open questions, in this work, we bring in new tools to understand the nature of extended-critical transitions. The rest of the paper is organized as follows. We briefly introduce the AAH Hamiltonian with p -wave pairing in Sec. II. Section III introduces the spectrum-averaged von Neumann entropy. We then provide evidence that such multipartite entanglement measure is well suited for characterizing the extended-critical transition and the fractal dimension of the critical phase. Section IV is devoted to the finite-size scaling (FSS) of GFSSs, and extracting the critical exponents that cannot be obtained from conventional scaling analysis. In Sec. V, we give a brief summary.

II. MODEL HAMILTONIAN

We consider the Hamiltonian for the AAH model with p -wave pairing in a quasiperiodically modulated potential,

$$H = \sum_{j=1}^N (-Jc_j^\dagger c_{j+1} + \Delta c_j c_{j+1} + \text{H.c.}) + \sum_{j=1}^N V_j \left(c_j^\dagger c_j - \frac{1}{2} \right), \quad (1)$$

where c_j^\dagger (c_j) is the fermionic creation (annihilation) operator at site j among total N lattice sites, J denotes the nearest-neighbor hopping amplitude, Δ characterizes the strength of p -wave superconducting pairing, and H.c. stands for the Hermitian conjugate. In certain contexts, the superconducting order parameter may appear in the mean-field approximation of the interacting AAH model [60]. Without losing generality, we assume $J = 1$ as an energy unit throughout the paper. The external potential in Eq. (1) is quasiperiodic, i.e., $V_j = V \cos(2\pi\alpha j + \phi)$, where $\phi \in [0, 2\pi)$ is a random phase and V is the amplitude of the potential with an irrational wave number α . A commonplace choice for α is the inverse

golden ratio $\alpha = (\sqrt{5} - 1)/2$. The boundary condition is imposed as $c_{N+1} = \sigma c_1$, where $\sigma = 1, -1$, and 0 corresponding to periodic, antiperiodic, and open boundary conditions, respectively. The Hamiltonian describes the Kitaev p -wave superconducting model for $\alpha = 0$, while the model reduces to the celebrated Aubry-André model when $\Delta = 0$, which undergoes a localization-delocalization transition at $V = 2J$ [35–37]. Once the p -wave pairing is turned on, the symmetry breaking from $U(1)$ down to \mathbb{Z}_2 leads to the emergence of the CP sandwiched between these two phases [46,47,61]. Upon increasing the Aubry-André potential strength V , the system undergoes continuous transitions from the CP to the EP for $V_{c1} = 2|\Delta - J|$ and from the CP to the LP for $V_{c2} = 2|\Delta + J|$ [44,46]. Analogously to the case of $\Delta = 0$, all the eigenstates of the Hamiltonian in Eq. (1) with a generic Δ undergo two transitions simultaneously. For $\Delta = \pm 1$, the model will be equivalent to the quasiperiodic Ising model [29,62], in which the phase transition occurs only between critical and localized phases [48,57]. The FSS of generalized participation indicates that the correlation-length exponent $\nu = 1$ across both transitions for all irrational α [44], consistent with the Harris criterion [63], which imposes that $\nu < 2$ for phase transitions in the presence of incommensurate modulation. In the numerical treatment on finite lattices, it is convenient to replace the inverse golden ratio with a rational approximant being a ratio of two Fibonacci numbers, $\alpha = F_{\ell-1}/F_\ell$, and thus the diagonal Aubry-André potential has periodicity of F_ℓ sites in order to allow for the use of periodic boundary conditions, where F_ℓ is the ℓ th Fibonacci number. As noted before [64–66], the sequence of denominators F_ℓ breaks into three subsequences. As we will show, each subsequence is characterized with a separate scaling function. The lattice system N can be chosen as ζ supercells, where $N = \zeta F_\ell$. For simplicity, we consider $\zeta = 1$ and two-subsequence odd sizes in the following, i.e., $F_{3\ell+1} = 21, 55, 233, 987, \dots$, and $F_{3\ell+2} = 89, 377, 1597, 6765, \dots$. In this respect, the Hamiltonian (1) can be diagonalized through a canonical Bogoliubov-de Gennes (BdG) transformation by introducing quasiparticle operators η_k and η_k^\dagger , which is a linear combination of an electron and hole:

$$\eta_k = \sum_{j=1}^N (u_{k,j} c_j + v_{k,j} c_j^\dagger), \quad \eta_k^\dagger = \sum_{j=1}^N (u_{k,j}^* c_j^\dagger + v_{k,j}^* c_j), \quad (2)$$

where $u_{k,j}$ and $v_{k,j}$ denote electron and hole amplitudes of Bogoliubov quasiparticle at site j for the k th eigenstate. For a given normalized wave ($\sum_j |u_{k,j}|^2 + |v_{k,j}|^2 = 1$), η_k and η_k^\dagger satisfy the anticommutation relation:

$$\{\eta_k, \eta_{k'}^\dagger\} = \delta_{kk'}, \quad \{\eta_k, \eta_k\} = \{\eta_k^\dagger, \eta_k^\dagger\} = 0. \quad (3)$$

In the Nambu representation, the Schrödinger equation $H|\psi_k\rangle = \epsilon_k|\psi_k\rangle$ can be recast into a $2N \times 2N$ matrix form as [46]

$$\begin{pmatrix} A & B \\ -B^* & -A^T \end{pmatrix} \begin{pmatrix} u_k \\ v_k \end{pmatrix} = \epsilon_k \begin{pmatrix} u_k \\ v_k \end{pmatrix}, \quad (4)$$

where $A = -J(\delta_{i+1,j} + \delta_{i-1,j}) + V_i \delta_{i,j}$, $B = -\Delta(\delta_{i+1,j} - \delta_{i-1,j})$, $u_k^T = (u_{k,1}, \dots, u_{k,N})$, and $v_k^T = (v_{k,1}, \dots, v_{k,N})$. The matrix elements for the boundary terms $A_{N,1} = A_{1,N} = -\sigma J$, $B_{N,1} = -B_{1,N} = -\sigma \Delta$.

The BdG Hamiltonian in Eq. (4) obeys an imposed particle-hole symmetry, implying $\eta_k(\epsilon_k) = \eta_k^\dagger(-\epsilon_k)$. The excitation spectrum ϵ_k is a solution of the secular equation $\det[(A+B)(A-B) - \epsilon_k^2] = 0$. The energy levels appear in $\pm\epsilon_k$ conjugate pairs, with $\epsilon_k \geq 0$, except the zero-energy mode, which is self-conjugate. In terms of the operators η_k and η_k^\dagger , the Hamiltonian in Eq. (1) can be diagonalized as

$$H = \sum_{k=1}^N 2\epsilon_k \left(\eta_k^\dagger \eta_k - \frac{1}{2} \right), \quad (5)$$

where ϵ_k are single-particle energies in ascending order, i.e., $\epsilon_1 \leq \epsilon_2 \leq \dots \leq \epsilon_N$. The ground state of H is the Bogoliubov vacuum state $|\psi_g\rangle$ annihilated by all η_k ($k = 1, \dots, N$), i.e., $\eta_k |\psi_g\rangle = 0$, with an energy $E_g = -\sum_{k=1}^N \epsilon_k$. In the spirit of the Ginzburg-Landau scenario of continuous phase transitions, the characterization of quantum phase transitions in many-body systems has been traditionally based on a suitable order parameter Q , whose expectation value in the ordered phase is finite while it becomes exactly zero at criticality: $Q \sim |V - V_c|^{\beta_Q}$, where the exponent β_Q of this power law is dubbed as the order parameter critical exponent. The scaling exponents reflect the universality class of the theory, which is independent of the microscopic details of the model but depends only on global properties such as the symmetries and dimensionality of the Hamiltonian. The asymptotic behavior of critical phenomena corresponding to the thermodynamic limit can be retrieved using FSS [67]:

$$Q(N, V) = N^{-\beta_Q/\nu} \tilde{Q}(|V - V_c|N^{1/\nu}), \quad (6)$$

where ν characterizes the divergence of the correlation length and \tilde{Q} is a universal scaling function [68]. However, it remains a systematic challenge to identify an explicit local order parameter in random models and analog quasiperiodic systems. There is no explicit symmetry breaking associated with a local order parameter, and therefore it has no experimental signature in the ground-state energy or its derivatives. Over recent years, an alternative approach to understand quantum criticalities and the associated universality exploits the information content stored in the many-body degrees of freedom of a quantum system. In the following, we investigate the quantum criticality of the AAH model from the quantum information perspective. Quantum entanglement and fidelity susceptibility have been widely exploited in the research of various phase transitions without any prior knowledge of order parameters. Specifically, these information measures can reconcile seemingly unrelated behaviors in different branches of physics ranging from condensed matter physics to gravitational physics. It is interesting to note that quantum entanglement may be used to shed light on the black-hole information paradox regarding the anti-de Sitter/conformal field theory (AdS/CFT) correspondence, which was initially proposed due to the scaling behavior of entropy in black holes [69], while the fidelity susceptibility is dual to the volume of codimension one time slice in AdS spacetime [70]. Therefore, it is quite intriguing to check whether the FSS of the universal order parameters applies also in the quasiperiodic models.

III. VON NEUMANN ENTROPY

The first attempt along this vein focuses on the study of quantum entanglement. As a pure quantum concept with no classical counterpart, entanglement describes nonlocal correlations between the constituents of quantum systems. During the last decade, there has been an increasing interest in the entanglement properties of quantum systems, in particular in specifying quantum criticalities [71–73]. Quantum entanglement is especially suitable for characterizing phases that lack explicit local order parameters, such as topological states [74,75], spin liquids [76], and topological order [77]. It is noted that the outcomes of entanglement witness rely heavily on the possible partition of the Hilbert space, the so-called entanglement cuts, which can be performed on real space, momentum space, or internal degrees of freedom of fermions [78]. The many-body entanglement entropy can be formulated in terms of the covariance matrix restricted to the subsystem, which is the manifestation of the large gaps in the single-particle energy spectrum and very sensitive to the subband structure of the spectrum [79]. Despite the extensive literature on the criticality measures related to wave function, there have been only very few works exploring the entanglement entropy in the AAH model near criticality [80–83]. The spatial entanglement entropy of a quantum state is a common thread for analyzing the delocalized-localized transitions. In the delocalized phase, where the wave function is extended over many sites, one may expect considerable correlation spreads in the system and thus the entanglement entropy therein is larger than that in the localized phase. The single-particle states show an interesting multifractal behavior extending to all length scales, which is reflected by the nonlinear dependence of the fractal dimensions D_q on q , $q \geq 0$, defined via the scaling of the q -order IPR:

$$D_q = \left\langle \frac{\ln \sum_j |\psi_{k,j}|^{2q}}{(1-q) \ln N} \right\rangle, \quad (7)$$

where $\langle \cdot \rangle$ denotes the average over all k th eigenstates. By performing the FSS of the mean IPR, the fractal dimensions $D_2 = 1$ and 0 characterize the self-similar behavior for the EP and the LP, respectively, whereas $0 < D_2 < 1$ implies multifractality in critical states. We are aware of the fact that the entanglement entropy has not yet been employed to analyze the multifractal structure in the AAH model with p -wave pairing, although an upper bound for the entanglement entropy for any eigenstate with a given fractal dimension was established [84].

To this end, we here conduct the analysis of the single-site entanglement entropy. For spinless noninteracting fermions in the AAH model, there are two local states at the j th site, i.e., $|1\rangle_j, |0\rangle_j$, corresponding to states with one and zero particles, respectively. Considering a generic eigenstate for Hamiltonian (1) that can be obtained by diagonalizing Eq. (4), the single-site reduced density matrix $\rho_{k,j}$ for the k th eigenstate at the j th site can be written as

$$\rho_{k,j} = |u_{k,j}|^2 |1\rangle_j \langle 1|_j + (1 - |u_{k,j}|^2) |0\rangle_j \langle 0|_j. \quad (8)$$

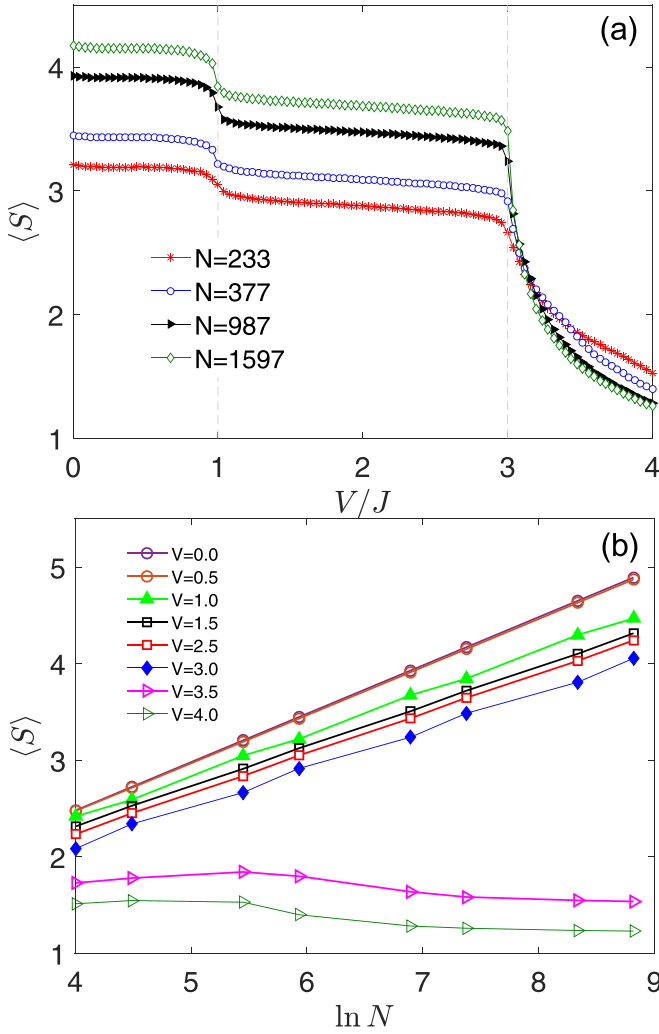


FIG. 1. (a) The SAE E $\langle S \rangle$ versus the incommensurate potential strength V for various system sizes N . (b) The scaling of $\langle S \rangle$ for different V . Here periodic boundary conditions are used with $\Delta = 0.5$, $\phi = 0$.

Consequently, the single-site von Neumann entropy associated with site j can be expressed as

$$S_{k,j} = -|u_{k,j}|^2 \ln |u_{k,j}|^2 - (1 - |u_{k,j}|^2) \ln(1 - |u_{k,j}|^2). \quad (9)$$

For quasiperiodic systems, the spatial von Neumann entropy for the k th eigenstate over different sites is given by

$$S_k = \sum_{j=1}^N S_{k,j}, \quad (10)$$

and the spectrum-averaged entanglement entropy (SAEE)

$$\langle S \rangle = \frac{1}{2N} \sum_{k=1}^{2N} S_k. \quad (11)$$

Figure 1(a) shows the SAEE as a function of the incommensurate potential V for various system sizes N with $\Delta = 0.5$ and $\phi = 0$. One can observe that $\langle S \rangle$ displays sudden falls at $V_{c1} = 2|J - \Delta|$ and $V_{c2} = 2|\Delta + J|$. It is clear that $\langle S \rangle$ has a lower value in the LP than that in the delocalized phases.

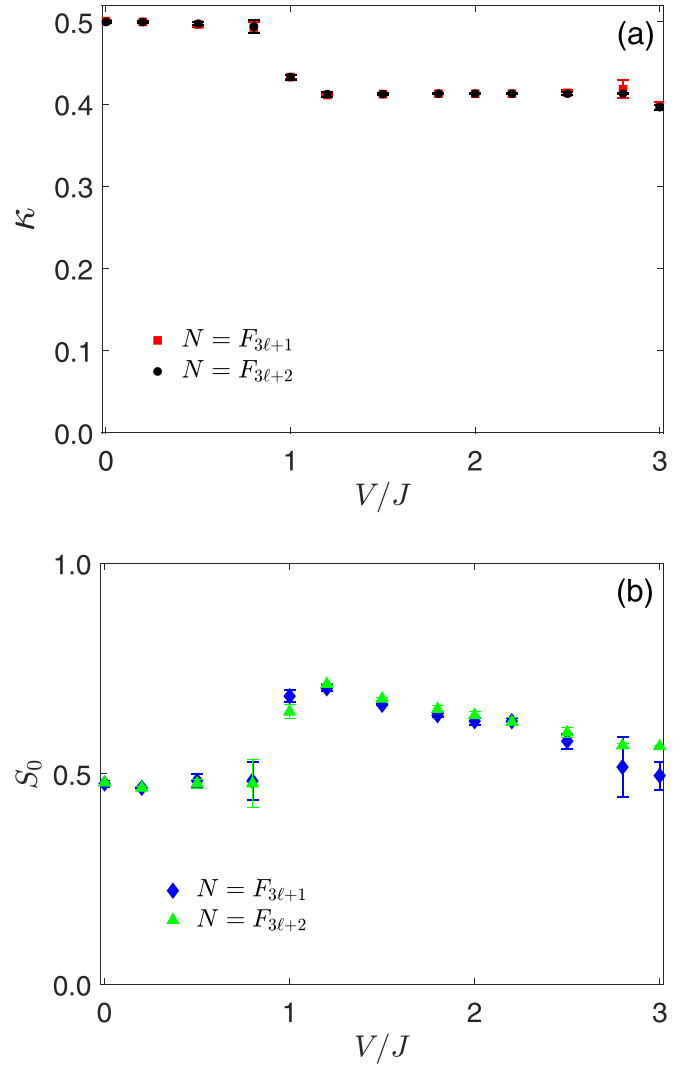


FIG. 2. The fitted values of (a) κ and (b) S_0 in Eq. (13) for $N = F_{3\ell+1}$ and $F_{3\ell+2}$. Here periodic boundary conditions are used with $\Delta = 0.5$, $\phi = 0$.

In the EP and the CP, $\langle S \rangle$ shows a monotonic increase as the system sizes N increase, in stark contrast to the decreasing tendency in the LP. We then assume an *Ansatz* of the FSS for $\langle S \rangle$ in the vicinity of V_{c1} under investigation [67]:

$$\langle S \rangle = N^{\beta_S/\nu} \tilde{S}(|V - V_{c1}|N^{1/\nu}), \quad (12)$$

where β_S is the corresponding critical exponent, and \tilde{S} is a universal scaling function [68].

Figure 1(b) reveals that the SAEE in the delocalized phases follows the law

$$\langle S \rangle = \kappa \ln N + S_0, \quad (13)$$

with the asymptotic prefactor κ and the nonuniversal residual entropy S_0 . The fitted values κ and S_0 for different quasiperiodic potential strengths. For $V < V_{c1}$, $\langle S \rangle$ has a negligible dependence on V . A close inspection for N up to 6765 finds $\kappa_{EP} \approx 0.500$, which is almost identical with the mean spectral exponent $\alpha_0 = 0.5$ [85]. Especially for the homogeneous case $V = 0$, the system is simply a single-band Kitaev Hamiltonian. The spatial entanglement entropy

becomes equivalent to the Meyer-Wallach measure of multipartite global entanglement [86,87], while for $V_{c1} < V < V_{c2}$, the overall logarithmic scaling of $\langle S \rangle$ is decorated with an oscillation of a two-subsequence period. One has to fit the data for $N = F_{3\ell+1}$ and $N = F_{3\ell+2}$ separately. Despite wide fluctuations, the fitted slope is nearly a constant as $\kappa_{CP} \approx 0.414$. In fact, in the limit $q \rightarrow 1$, Eq. (7) provides important information on the effective dimension of the support set for the mean entanglement entropy in Eq. (11), which scales as $\langle S \rangle \sim N^{D_1}$ given by $D_1 = \kappa_{CP}/\kappa_{EP}$ in the Nambu space [88]. We note that the value is close to the maximal fractal dimension $D_2 \approx 0.82$ in the ground state of the Harper model [85]. The fluctuations are reflected in the fitted values of S_0 , which varies with V . One observes $\langle S \rangle$ first grows and then declines until saturating to finite values in the limit $N \rightarrow \infty$, thus yielding $\kappa_{LP} \rightarrow 0$ in Eq. (13) for localized wave functions. We can anticipate $\langle S \rangle \approx 0$ in the extremely localized phase for $V \rightarrow \infty$. In the localized phase, all one-particle eigenstates are localized on a length N_{loc} . For lengths larger than the localization length N_{loc} , the wave function consists of a single isolated structure and its correlation dimension D_2 is zero. One may expect that in large systems $N \gg N_{loc}$ the length scale is set by the localization length N_{loc} rather than the system size N ; the entanglement entropy in Eq. (13) may be rewritten as $\langle S \rangle = \kappa_{loc} \ln N_{loc} + S_0$ [89]. The *Ansatz* is expected to deteriorate when the diverging localization length becomes comparable with the system size. It is evident that Eq. (13) implies that $\beta_S = 0$ in the vicinity of the EP-CP transition. To refine more critical exponents, we have to resort to the first derivative of the SAAE as

$$d\langle S \rangle/dV = N^{(1+\beta_S)/\nu} \tilde{S}'(|V - V_{c1}|N^{1/\nu}), \quad (14)$$

where $\tilde{S}'(\cdot)$ is the first derivative with respect to the argument. Using the *Ansatz* in Eq. (14), we perform the FSS for an odd number of system sizes around the critical point V_{c1} . As shown in Fig. 3(a), the minima of $d\langle S \rangle/dV$ become deeper and the corresponding positions of the valleys V_m converge toward the critical points with increasing the system sizes. A careful analysis easily identifies that V_m are above V_{c1} for $N = F_{3\ell+1}$, while they are below V_{c1} for $N = F_{3\ell+2}$. The two-subsequence behavior of $d\langle S \rangle/dV$ can be manifested by taking the logarithm on both sides of the *Ansatz* (14),

$$\ln d\langle S \rangle/dV = [(1 + \beta_S)/\nu] \ln N + \ln \tilde{S}'(|V - V_{c1}|N^{1/\nu}). \quad (15)$$

To be concrete, the power-law relations can be further identified as

$$\left| \left(\frac{d\langle S \rangle}{dV} \right)_{\min} \right| = \tilde{S}'(0) N^{(1+\beta_S)/\nu}, \quad (16)$$

$$|V_m - V_{c1}| \propto N^{-1/\nu}. \quad (17)$$

The linear scaling relations are confirmed by the numerical fittings in the insets of Fig. 3(a). The extrema of $d\langle S \rangle/dV$ satisfy $\ln |(d\langle S \rangle/dV)_{\min}| = (0.953 \pm 0.095) \ln N - (4.552 \pm 0.608)$ and $\ln |(V_{c1} - V_m)| = (-0.962 \pm 0.117) \ln N + (0.458 \pm 0.169)$ for $N = F_{3\ell+1}$, suggesting $\beta_S = 0$, $\nu = 1.000$. Similarly, for $N = F_{3\ell+2}$ the linear fit to the log-log plot yields $\ln |(d\langle S \rangle/dV)_{\min}| = (0.980 \pm 0.027) \ln N - (4.147 \pm 0.183)$ and $\ln |(V_{c1} - V_m)| = (-0.998 \pm 0.010) \ln N + (1.378 \pm 0.071)$. Apparently the estimated values of critical exponents agree well with each other, which are independent

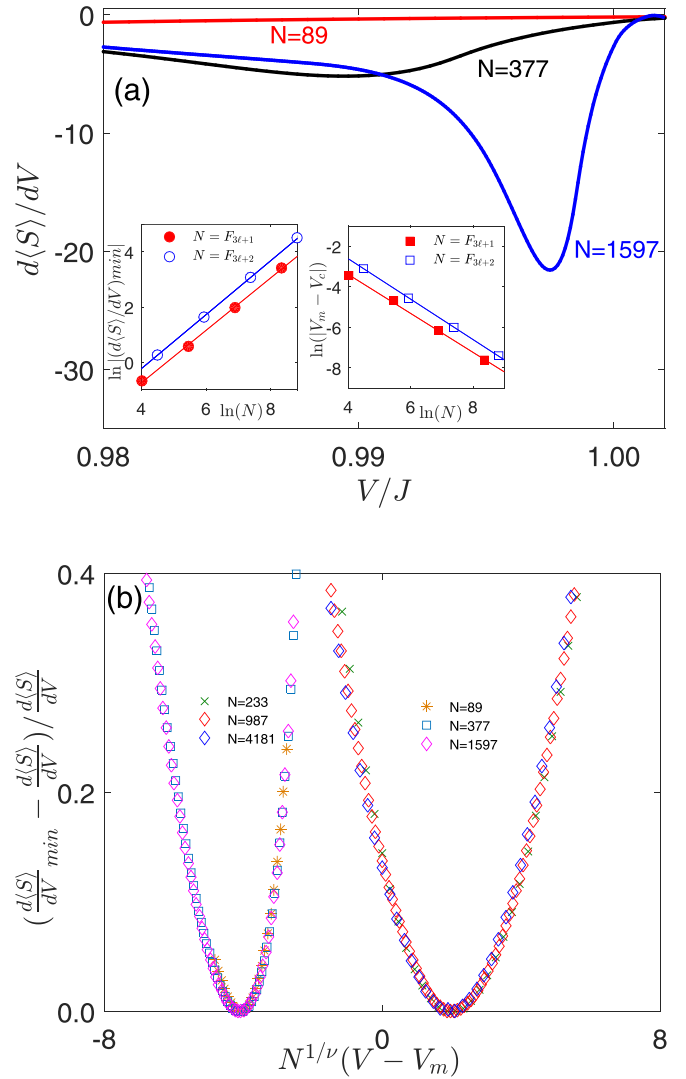


FIG. 3. (a) $d\langle S \rangle/dV$ with respect to V with the system sizes $N = 89, 377, 1597$. The left and right insets show the scaling behavior of $\ln |(d\langle S \rangle/dV)_{\min}|$ and $\ln |(V_m - V_{c1})|$ for N . (b) $[(d\langle S \rangle/dV)_{\min} - (d\langle S \rangle/dV)] / (d\langle S \rangle/dV)$ as a function of the scaled variable $N^{1/\nu}(V - V_m)$. All curves for odd number of lattice sizes collapse into two separate curves when we choose the correlation-length critical exponent $\nu = 1.000$. Here $\Delta = 0.5$ and $\phi = 0$.

of the Fibonacci subsequence. Figure 3(b) shows that the scaled $d\langle S \rangle/dV$ near criticality for different values of N superposes onto two separate scaling functions when the correlation-length critical exponent $\nu = 1.000$ is chosen. The perfect data collapse validates the scaling relation in Eq. (14).

IV. GENERALIZED FIDELITY SUSCEPTIBILITY

It has been shown that the multipartite entanglement dictates not only the position of critical points but also the correlation-length critical exponent ν . However, according to the Widom scaling hypothesis [90], there are generally two independent critical exponents and thus a second independent critical exponent plays a decisive role in determining the universality class. We then endeavor to apply GFS to obtain the dynamical exponent z , which has been successfully

developed in the CP-LP transition of the p -wave-paired AAH model [59]. The fidelity susceptibility has been regarded as a vital tool to identify critical points by measuring the rate of change for a given state after a sudden infinitesimal quench of the tuning parameter [91]. It should be emphasized that the ground-state fidelity susceptibility is unable to witness the EP-CP transition, as is shown in Appendix A. As a result, the GFS associated with an eigenstate $|\psi_k\rangle$ has a visible implication on the response of the system, which is given by a summation form [92,93]

$$\chi_{2r+2}^{(k)} = \sum_{k' \neq k} \frac{|\langle \psi_{k'} | \partial_V \hat{H} | \psi_k \rangle|^2}{(\epsilon_{k'} - \epsilon_k)^{2r+2}}, \quad (18)$$

where $|\psi_{k'}\rangle$ and $\epsilon_{k'}$ correspond to the k' th eigenstate and eigenvalue of Hamiltonian (1), respectively. In parallel with Eq. (11), it is tempting to speculate that the spectrum-averaged fidelity susceptibility serves as an effective tool for characterizing the quantum criticality in the AAH model. In Appendix B, we unveil that there is no qualitative difference between the average fidelity susceptibility and the typical fidelity susceptibility.

In this following, we focus on the GFS of the lowest eigenstate $|\psi_1\rangle$. In this case, Eq. (18) reduces respectively to the second derivative of $\chi_1 \equiv \partial^2 \epsilon_1 / \partial V^2$ for $r = -1/2$ and the standard fidelity susceptibility $\chi_2 \equiv \langle \partial_V \psi_1 | \partial_V \psi_1 \rangle - \langle \partial_V \psi_1 | \psi_1 \rangle \langle \psi_1 | \partial_V \psi_1 \rangle$ for $r = 0$ [91]. Accordingly, the GFS of a finite system with size N in the neighborhood of V_{c1} shall obey the universal scaling form [94]:

$$\chi_{2r+2} = N^{\beta_r} \tilde{\chi}_r(|V - V_{c1}|N^{1/\nu}), \quad (19)$$

where $\beta_r \equiv 2/\nu + 2zr$ is the critical adiabatic dimension, and $\tilde{\chi}_r$ is a regular universal scaling function of the GFS of order $2r + 2$. With increasing the system sizes N , the peaks of GFS become sharper and the peak position V_m approaches the critical point. However, in the actual calculation, V_m is quite close to V_{c1} for a moderate N owing the accelerated convergence of the fidelity susceptibility and thus Eq. (17) is beyond the current numerical accuracy. The determination of critical exponents can be only recapitulated through the following relation:

$$\chi_{2r+2}(V_m) = \tilde{\chi}_r(0)N^{\beta_r}. \quad (20)$$

Considering the fidelity susceptibility is proportional to the system size far away from the critical point, we show the fidelity susceptibility per site χ_2/N as a function of the incommensurate potential V for $\Delta = 0.5$ in Fig. 4(a). The peaks of the fidelity susceptibility around the critical point $V_{c1} = 1.0$ become more pronounced for increasing the system sizes N . The maxima of χ_2 show a power-law divergence, manifested by a linear fit between the maximum of $\ln \chi_2$ and $\ln N$. We can also observe a two-subsequence behavior and the fitted slopes give rise to $\beta_0 \equiv 2/\nu = 1.991 \pm 0.007$ (1.972 ± 0.035) for $N = F_{3\ell+1}$ ($F_{3\ell+2}$) according to Eq. (20). Therefore, the retrieved correlation-length exponent corresponds to $\nu = 1.005 \pm 0.018$ (1.014 ± 0.018) for $N = F_{3\ell+1}$ ($F_{3\ell+2}$). To coin the single-parameter scaling hypothesis in Eq. (19), we also plot the rescaled fidelity susceptibility $[\chi_2(V_m) - \chi_2(V)]/\chi_2(V)$ as a function scaled variable $N^{1/\nu}(V - V_m)$. When $\nu = 1.000$ is chosen, the curves with distinct system

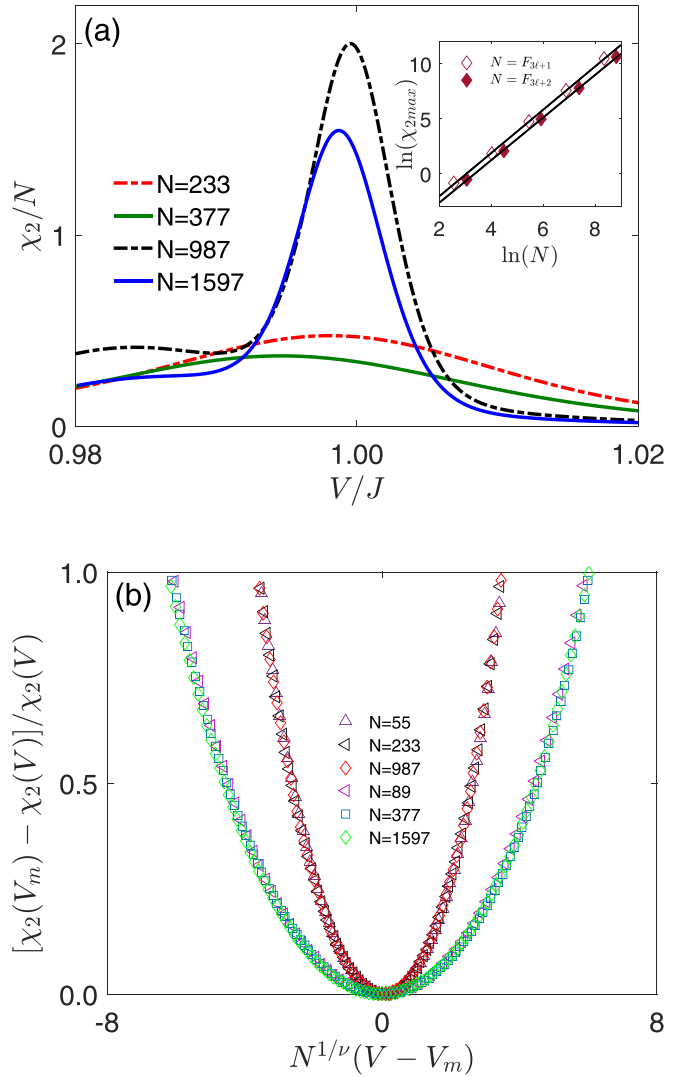


FIG. 4. (a) The fidelity susceptibility per site χ_2/N as a function of the incommensurate potential strength V around $V_{c1} = 1.0$. The inset shows the scaling behavior of the maxima versus the system sizes for $N = F_{3\ell+1}$: 13, 55, 233, 987, 4181 and $N = F_{3\ell+2}$: 21, 89, 377, 1597, 6765. (b) Scaled fidelity susceptibility $[\chi_2(V_m) - \chi_2(V)]/\chi_2(V)$ as a function of the scaled variable $N^{1/\nu}(V - V_m)$. All curves collapse into two separate curves when we choose the correlation-length critical exponent $\nu = 1.000$. Here periodic boundary conditions are used with $\Delta = 0.5$, $\phi = 0$.

sizes in the vicinity of V_{c1} collapse onto two scaling functions, as are evinced in Fig. 4(b). In order to extract the dynamical exponent z of the transition between the EP and the CP, we further study higher-order GFSs. One can easily notice that χ_3 and χ_4 display much more divergent peaks than χ_2 in the vicinity of the critical point, showing that the higher-order GFSs are more efficient in spotlighting the pseudocritical points. The scaling behaviors between $\ln \chi_{3,max}$ and $\ln N$ are displayed in Fig. 5(a). According to Eq. (20), the linear fittings of the log-log plot give rise to $\beta_{1/2} \equiv 2/\nu + z = 5.607 \pm 0.009$ (5.607 ± 0.009) for $N = F_{3\ell+1}$ ($F_{3\ell+2}$), corresponding to the dynamical exponent $z \equiv \beta_{1/2} - \beta_0 = 3.616 \pm 0.002$ (3.615 ± 0.018). Subsequently, the fitting

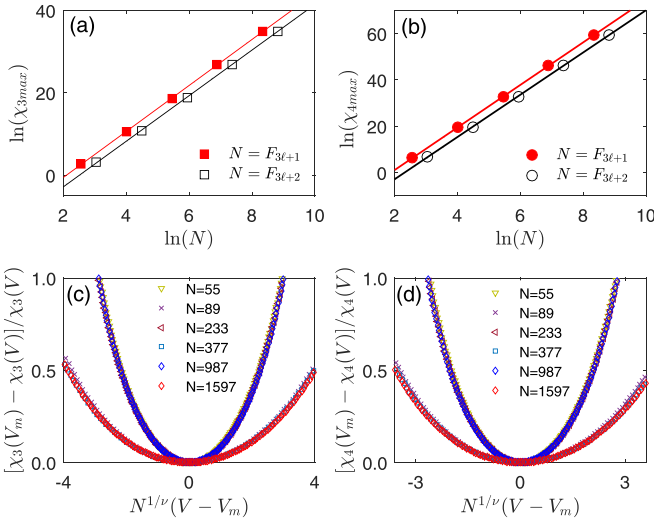


FIG. 5. Scalings of (a) $\chi_{3,\max}$ and (b) $\chi_{4,\max}$ with respect to system sizes N . Scaled fidelity susceptibilities (c) $[\chi_3(V_m) - \chi_3(V)]/\chi_3(V)$ and (d) $[\chi_4(V_m) - \chi_4(V)]/\chi_4(V)$ as a function of the scaled variable $N^{1/\nu}(V - V_m)$ for odd number of lattice sizes. All curves are collapsed into two separate scaling functions: one for $N = F_{3\ell+1}$ and the other for $N = F_{3\ell+2}$ when we choose the correlation-length critical exponent $\nu = 1.000$. Here we take periodic boundary conditions with $\Delta = 0.5$ and $\phi = 0$.

lines of $\ln \chi_{4,\max}$ with respect to $\ln N$ are exhibited in Fig. 5(b), whose slopes yield $\beta_1 \equiv 2/\nu + 2z = 9.220 \pm 0.007$ (9.201 ± 0.023) for $N = F_{3\ell+1}$ ($F_{3\ell+2}$), corresponding to $z \equiv (\beta_1 - \beta_0)/2 = 3.615 \pm 0.001$ (3.615 ± 0.006). The curves for χ_3 and χ_4 near the EP-CP transition can be separately rescaled onto two different universal curves for odd numbers of lattice sites with the same exponent $\nu = 1.000$, as seen in Figs. 5(c) and 5(d). Since there is no gap scaling of ϵ_1 around V_{c1} , a relevant spectral gap can be defined as $\epsilon_r \equiv \epsilon_3 - \epsilon_2$. Fitting ϵ_r with respect to the system size N yields $z = 3.610 \pm 0.017$ (3.617 ± 0.022) for $N = F_{3\ell+1}$ ($F_{3\ell+2}$), as is revealed in Fig. 6(a). As such, the extracted value of the dynamical exponent z is in perfect agreement with the GFS scaling.

Subsequently, we proceeded to extract ν and z for different Δ utilizing the same strategy in Fig. 6(b). It is found that the critical-length exponent $\nu \approx 1.000$ and the dynamical exponent $z \approx 3.610$ are almost unchanged for varying Δ . We note that the difference of estimated values of both critical exponents between two Fibonacci subsequences of system sizes is negligible. Numerical analysis shows that the phase transition at $V_{c1} = 2|\Delta - J|$ belongs to a different universality class from the quasiperiodic Ising universality at V_{c2} with $\nu \simeq 1.000$, $z \simeq 1.388$ [59].

V. DISCUSSION AND SUMMARY

In this paper, we pose an important and less understood question relating to the universality class of the transition from the extended phase to the critical phase in the Aubry-André-Harper (AAH) model with p -wave pairing, which are both gapped under periodic boundary conditions. Traditionally, for a conventional quantum many-body system described by a local Hamiltonian, it is accepted that two gapped ground states

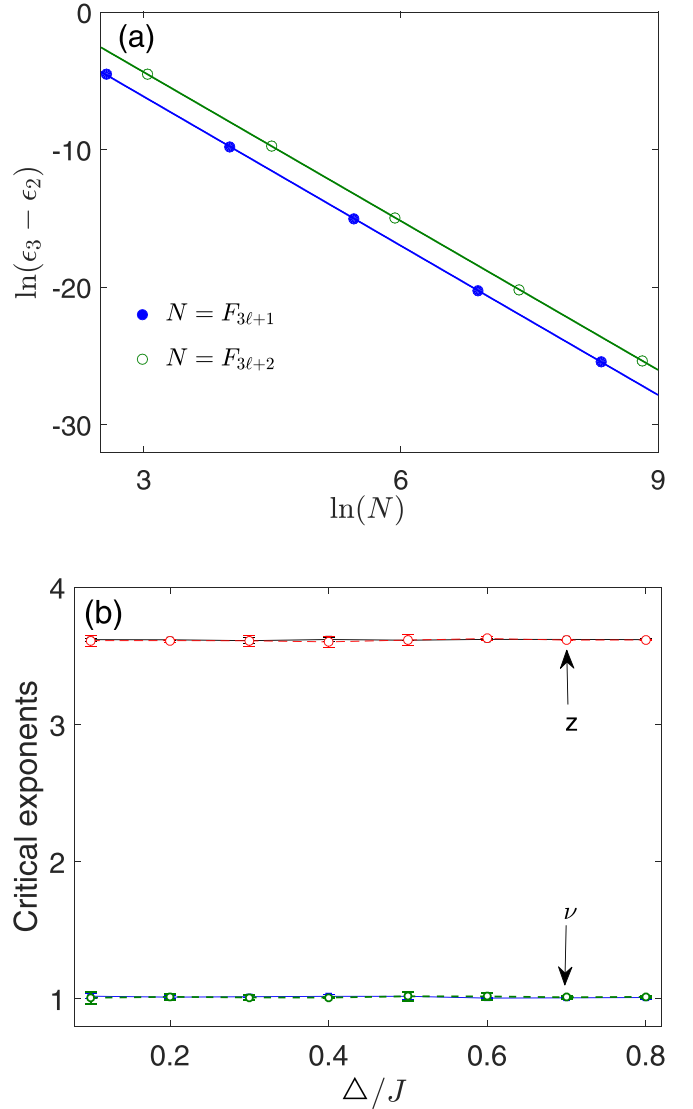


FIG. 6. (a) The scaling behavior of the minima of $\epsilon_r \equiv \epsilon_3 - \epsilon_2$ versus N around the critical point $V_{c1} = 1.0$ for $\Delta = 0.5$. (b) The fitted values of critical exponents ν and z as Δ varies for $N = F_{3\ell+1}$ (solid symbols) and $F_{3\ell+2}$ (open symbols). Here we take periodic boundary conditions with $\phi = 0$.

that are connected without gap closing are generally considered to belong to the same quantum phase. The undecidability of local order parameters exerts an obstacle of comprehending the nature of the transition between the extended phase and the critical phase. Nevertheless, this phase transition is reflected in the spatial variation of the wave function and can only be captured by quantities that probe its extended or localized nature, such as the inverse participation ratio (IPR), the bandwidth distribution, and the level spacing distribution. To this end, we investigate the quantum criticality and universality in the AAH model from the perspective of information measures. In particular, we can extract the universal information through the finite-size scaling of these measures, an impressive result given the limited number of system sizes in the quasiperiodic systems, whose system sizes are rapidly growing three-subsequence Fibonacci numbers.

The extended phase and the critical phase are characterized by a logarithmic divergence of spectrum-averaged entanglement entropy (SAEE) with the coefficients independent of the incommensurate modulation within each phase, in analogy to the bipartite entanglement entropy in the gapless phase. Notice that many-body entanglement entropy in two gapped phases admits the area-law scaling in this case. In the extended state the prefactor is found to be equal to that of the conformally invariant homogeneous system, while in the critical state the prefactor is reduced to a smaller value, which can mark the fractal dimension. Meanwhile, the SAEE will saturate toward a constant for localized states. It becomes evident that the phase transitions in the AAH model are not thermodynamic phase transitions due to the absence of an explicit symmetry breaking. The transition between the extended phase and the critical phase can be ascribed to a reduction of the effective dimensionality across the critical point. We formulate Widom-like scaling *Ansätze* for the SAEE and its derivative, which are corroborated by an acceptable collapse for odd number of lattice sizes with a properly chosen correlation-length critical exponent ν . The numerical results indicate that the multipartite entanglement can provide us a deep understanding of critical phenomena in quasiperiodic systems. Furthermore, we show that the eigenstate generalized fidelity susceptibility (GFS) proves to be an accelerated method for identifying the location of critical points. More importantly, the versatility in GFSs of different orders poses an efficient avenue for retrieving the dynamical critical exponent z , which is unable to be obtained from nonclosing gap and standard fidelity susceptibility across the extended-critical transition. The GFSs in the vicinity of the critical point V_{c1} scale onto two separate scaling functions for each subsequence of odd system sizes N with $\nu \simeq 1.000$ and $z \simeq 3.610$. The extracted critical exponents are different from ones of the critical-localized transition point V_{c2} , i.e., $\nu \simeq 1.000$ and $z \simeq 1.388$.

Our work is interesting from various points of view. First, to the best of our knowledge, the critical exponents and the universal scaling analysis of the extended-critical transition in the p -wave-paired AAH model and other variants have not been retrieved yet. Second, we find that multipartite entanglement serves as a good indicator of phase transitions with interesting scaling behavior, which can recapitulate the fractal dimension. Third, we develop the strategy in terms of GFSs to analyze the critical phenomena in quasiperiodic systems and prove that the eigenstate GFS plays an irreplaceable role in describing the phase transition without gap closing. We emphasize that the phase transitions under consideration here, which cannot be diagnosed by the quantities associated with the many-body ground state, occur at the level of a single eigenstate in noninteracting systems. Last but not least, the rapid progress in quantum simulation sheds light on the experimental measurement of the correlation-length exponent ν and the dynamical exponent z with a finite number of ultracold atoms. For instance, z and ν may be extracted from specific-heat exponent α according to the hyperscaling relation $(d+z)\nu = 2 - \alpha$ or through the Kibble-Zurek exponent $\mu = \nu/(1 + \nu z)$ [40,95]. Thus, the scaling hypothesis provides a unified and comprehensive description of universal order parameters, which is propitious for extracting the as-

sociated universal information from limited system sizes of quasiperiodic quantum critical points. Our work paves a new routine of exploiting quantum criticality and universality in quasiperiodic and disordered systems. As a possible future direction, the present investigations could be extended to various generalized AAH models. We expect that the universality of the extended-critical transition may preserve and in particular the scaling analysis should hold in generalized AAH models, which even exhibit a mobility edge in the single-particle spectrum.

ACKNOWLEDGMENTS

This work is supported by the National Natural Science Foundation of China (NSFC) under Grant No. 12174194, the startup fund of Nanjing University of Aeronautics and Astronautics under Grant No. 1008-YAH20006, the Top-Notch Academic Programs Project of Jiangsu Higher Education Institutions (TAPP), and stable supports for basic institute research under Grant No. 190101.

APPENDIX A: GROUND-STATE FIDELITY SUSCEPTIBILITY IN FREE FERMI SYSTEMS

Equation (1) describes a quadratic Hamiltonian for quasifree spinless fermions that in general is given by

$$H = \sum_{i,j=1}^N c_i^\dagger A_{ij} c_j + \frac{1}{2} \sum_{i,j=1}^N (c_i^\dagger B_{ij} c_j^\dagger + c_j B_{ij} c_i), \quad (\text{A1})$$

where A (B) is a symmetric (antisymmetric) real $N \times N$ matrix, i.e., $A^T = A$, $B^T = -B$. The Hamiltonian (A1) can be rewritten in the more compact form as $H = (\Psi^\dagger C \Psi + \text{Tr}A)/2$, where $\Psi^\dagger = (c_1^\dagger, \dots, c_N^\dagger, c_1, \dots, c_N)$, $\Psi = (c_1, \dots, c_N, c_1^\dagger, \dots, c_N^\dagger)^T$, and $C = \sigma_z \otimes A + i\sigma_y \otimes B$. In this case, the diagonalization of Eq. (A1) can be implemented efficiently, as it involves operations in the Nambu space of dimension N^2 , much less than the dimension 2^N of the full Hilbert space.

We consider a linear transformation $\Psi' = V\Psi$, where $V = \mathbb{1}_2 \otimes u + \sigma_x \otimes v$ is orthogonal, with u, v being real matrices. The transformation is canonical due to the preservation of the anticommutation relations:

$$uu^T + vv^T = \mathbb{1} \quad \text{and} \quad uv^T + (uv^T)^T = 0. \quad (\text{A2})$$

Under the real canonical transformations, the Hamiltonian becomes $H = (\Psi'^\dagger C' \Psi' + \text{Tr}A)/2$, where the eigenvalue matrix $C' = VCV^T = \sigma_z \otimes \Lambda$ with the $N \times N$ positive-semidefinite diagonal matrix $\Lambda = \text{diag}(\Lambda_1, \dots, \Lambda_N)$. Here the fact that the eigenvalues of C appear in pairs of real numbers of opposite sign is guaranteed by the imposed particle-hole symmetry in the Nambu representation.

In fact, all information of Eq. (A1), including ground-state properties, can be decoded from an N^2 -dimensional auxiliary real matrix $Z \equiv A - B$ [96–98]. One can thus find that $Z' = A' - B'$ satisfies the simple relation

$$Z' = (u + v)Z(u - v)^T. \quad (\text{A3})$$

One then has $C' = \sigma_z \otimes A' + i\sigma_y \otimes B'$, so that $A' = \Lambda$, $B' = 0$ and hence $Z' = A' - B' = \Lambda$. From Eq. (A3), by defining

$\Phi \equiv u + v$ and $\Psi \equiv u - v$, one finally gets the important equations

$$\Phi Z \Psi^T = \Lambda \quad \text{and} \quad \Psi Z^T \Phi^T = \Lambda. \quad (\text{A4})$$

Consequently, Φ , Ψ , and Λ are simply given by the singular value decomposition of $Z = \Phi^T \Lambda \Psi$. Due to the canonical conditions, the matrices Φ and Ψ must be orthogonal. Then we can derive straightforwardly the following relations $\Lambda \Psi = \Phi Z$, $\Lambda \Phi = \Psi Z^T$. As a consequence, Φ and Ψ can be calculated by diagonalizing ZZ^T or $Z^T Z$, given by

$$\Phi ZZ^T = \Lambda^2 \Phi, \quad \text{and} \quad \Psi Z^T Z = \Lambda^2 \Psi. \quad (\text{A5})$$

Note that Φ and Ψ cannot be calculated by diagonalizing ZZ^T and $Z^T Z$ independently because of Eq. (A4). After solving Eq. (A5) for orthogonal matrices Φ , Ψ and diagonal matrix Λ , one introduces $u \equiv (\Phi + \Psi)/2$ and $v \equiv (\Phi - \Psi)/2$, in terms of which the canonically transformed operators diagonalizing the Hamiltonian are defined by

$$\eta_k \equiv \sum_{j=1}^N (u_{k,j} c_j + v_{k,j} c_j^\dagger). \quad (\text{A6})$$

Finally, the Hamiltonian reads

$$H = \sum_{k=1}^N \Lambda_k \eta_k^\dagger \eta_k + E_0, \quad (\text{A7})$$

where $E_0 = \text{Tr}(A - \Lambda)/2$ is the ground-state energy with Λ_k being single-particle energies.

The ground state can be obtained by imposing the condition $\eta_k |\Psi_0\rangle = 0$, $\forall k$ [99]. Recalling the singular value decomposition of Z ,

$$Z = \Phi^T \Lambda \Psi = (\Phi^T \Lambda \Phi^*) (\Phi^T \Psi) = PT, \quad (\text{A8})$$

giving rise to the polar decomposition of Z such that $Z = PT$, where $P \equiv \sqrt{ZZ^\dagger} = \Phi^T \Lambda \Phi^*$ is a positive-semidefinite matrix and $T = \Phi^T \Psi$ is unitary. The ground state has an explicit BCS-like form in the case of even parity [99],

$$|g_Z\rangle = \mathcal{N} \exp \left(\frac{1}{2} \sum_{j,k=1}^N c_j^\dagger G_{jk} c_k^\dagger \right) |0\rangle, \quad (\text{A9})$$

where \mathcal{N} is a normalization factor, $|0\rangle$ is the fermionic vacuum ($c_j |0\rangle = 0$), and G is a real $N \times N$ antisymmetric matrix, which satisfies

$$uG + v = 0. \quad (\text{A10})$$

Note that Eq. (A10) is not always solvable, corresponding to cases where either the *Ansatz* (A9) does not hold or the ground-state parity is odd. We will put these exceptions on hold for the moment. We will assume Z is invertible and T is well defined in the following.

When P (and hence Z) is invertible, by using Eq. (A4) one can write $u = \Phi(\mathbb{1} + P_\Phi^{-1}Z)/2$, $v = \Phi(\mathbb{1} - P_\Phi^{-1}Z)/2$, with $P_\Phi \equiv \Phi^{-1}P\Phi$, so that if u is invertible one has

$$G = \frac{T - \mathbb{1}}{T + \mathbb{1}}, \quad (\text{A11})$$

where G is the Cayley transform of $T \equiv P_\Phi^{-1}Z$, which is the orthogonal part of the polar decomposition of Z . From

Eq. (A11), the orthogonality $T^T = T^{-1}$ readily implies the antisymmetry $G^T = -G$. The inverse Cayley transform then yields $T = (\mathbb{1} + G)/(\mathbb{1} - G)$, implying $\det T = 1$. We can then find that the spectrum of the real antisymmetric matrix G is given by complex conjugate pairs of purely imaginary eigenvalues.

With the above wisdom, we are ready to calculate the ground-state fidelity as

$$F(Z, \tilde{Z}) \equiv |\langle g_Z | g_{\tilde{Z}} \rangle|. \quad (\text{A12})$$

We give an explicit evaluation of the fidelity (A12) from the unitary matrix T , which can be further simplified into the following form by recognizing that (A9) is a fermionic coherent state [100]:

$$\begin{aligned} F(Z, \tilde{Z}) &= \frac{\det(\mathbb{1} + G^\dagger \tilde{G})^{1/2}}{\det(\mathbb{1} + G^\dagger G)^{1/4} \det(\mathbb{1} + \tilde{G}^\dagger \tilde{G})^{1/4}} \\ &= \sqrt{\left| \det \frac{\mathbb{1} + T^{-1} \tilde{T}}{2} \right|} = \sqrt{\left| \det \frac{T + \tilde{T}}{2} \right|}, \end{aligned} \quad (\text{A13})$$

where T and \tilde{T} are respectively the unitary matrices of $Z \equiv Z(V)$ and $\tilde{Z} \equiv Z(V + \delta V)$ for infinitesimally close parameters V and $V + \delta V$.

Using $\sqrt{\det(M)} = \det(\sqrt{M})$ and $\det(e^M) = e^{\text{Tr}(M)}$, Eq. (A13) can be further simplified as

$$\begin{aligned} F(Z, \tilde{Z}) &= \sqrt{\left| \det \frac{T + \tilde{T}}{2} \right|} \\ &= \exp \left\{ \text{Tr} \ln \left(\frac{1 + T^\dagger \tilde{T}}{2} \right)^{1/2} \right\} \\ &= \exp \left\{ \text{Tr} \ln \left(\frac{1 + T^\dagger (T + \delta T)}{2} \right)^{1/2} \right\} \\ &= \exp \left\{ \text{Tr} \ln \left(1 + \frac{T^\dagger \delta T}{2} \right)^{1/2} \right\} \\ &= \exp \left\{ \text{Tr} \frac{1}{2} \ln \left(1 + \frac{T^\dagger \delta T}{2} \right) \right\} \\ &\approx \exp \left\{ \text{Tr} \left[\frac{1}{4} (T^\dagger \delta T) - \frac{1}{16} (T^\dagger \delta T)^2 \right] \right\}, \end{aligned} \quad (\text{A14})$$

where $\delta T = \partial_V T dV$. The fidelity susceptibility is thus obtained by [91]

$$\chi_F(V) = \lim_{\delta V \rightarrow 0} \frac{-2 \ln F}{\delta V^2}. \quad (\text{A15})$$

To this end, Eq. (A15) can be rewritten in terms of the unitary matrix T as

$$\chi_F = \frac{1}{8} \|\partial_V T\|_F^2, \quad (\text{A16})$$

where $\|M\|_F \equiv \sqrt{\text{Tr}(MM^\dagger)}$ is the Frobenius norm. As is observed in Fig. 7, the fidelity susceptibility manifests divergent peaks at V_{c2} , while there is no anomaly across V_{c1} without gap closing.

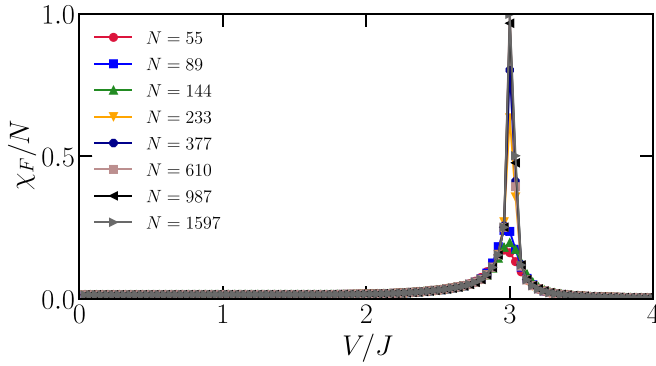


FIG. 7. The ground-state fidelity susceptibility χ_F/N as a function of the incommensurate potential strength V for different sizes N . Here periodic boundary conditions are used with $\Delta = 0.5$, $\phi = \pi$.

APPENDIX B: SPECTRUM-AVERAGED FIDELITY SUSCEPTIBILITY

It has been widely recognized that the fidelity susceptibility is extensive far away from criticality and superextensive at criticality with a vanishing small gap. In computing the spectrum-averaged fidelity susceptibility, the arithmetic mean is highly sensitive to large values of certain eigenstates, while the geometric mean gives rise to a more representative measure of the typical values of the physical quantity under consideration. Especially in the vicinity of the critical points, large fidelity susceptibilities skew the arithmetic average toward a greater value than the typical one. The arithmetic mean generally provides an upper bound for the geometric mean when taking the mean of a set of positive values and they become equal only when averaging over a constant set of values. We will define the average fidelity susceptibility as

$$\chi_2^{\text{ave}} \equiv \frac{1}{2N} \sum_{k=1}^{2N} \chi_2^{(k)}, \quad (\text{B1})$$

and the typical fidelity susceptibility as

$$\chi_2^{\text{typ}} \equiv \exp\left(\frac{1}{2N} \sum_{k=1}^{2N} \ln \chi_2^{(k)}\right). \quad (\text{B2})$$

We show both types of spectrum-averaged fidelity susceptibilities for the AAH model with p -wave pairing around $V_{c1} = 1.0$. We can observe similar behaviors in Fig. 8. Linear fits of local peaks reveal $\ln(\chi_{2,\text{max}}^{\text{typ}}) = (1.941 \pm 0.121) \ln N - (5.472 \pm 0.608)$ and $\ln(\chi_{2,\text{max}}^{\text{ave}}) = (1.957 \pm 0.038) \ln N - (5.260 \pm 0.388)$ for $N = F_{3\ell+1}$, while for $N = F_{3\ell+2}$, we have $\ln(\chi_{2,\text{max}}^{\text{typ}}) = (1.9678 \pm 0.054) \ln N - (4.994 \pm 0.295)$ and $\ln(\chi_{2,\text{max}}^{\text{ave}}) = (1.969 \pm 0.048) \ln N - (4.827 \pm 0.265)$, suggesting that the extracted coefficients of the slopes for the correlation-length

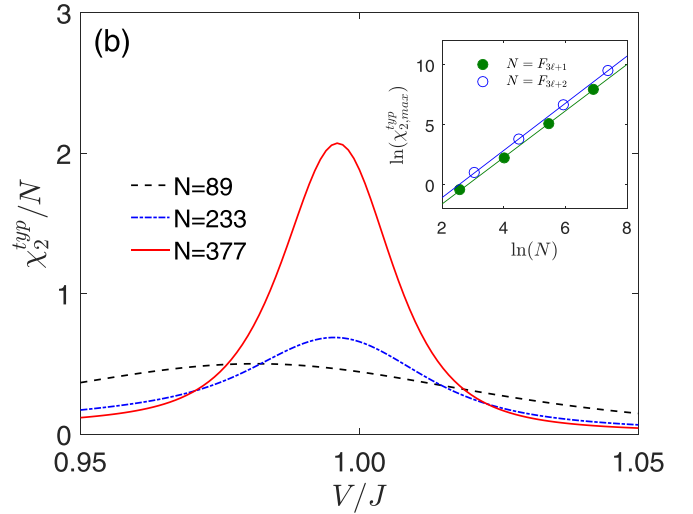
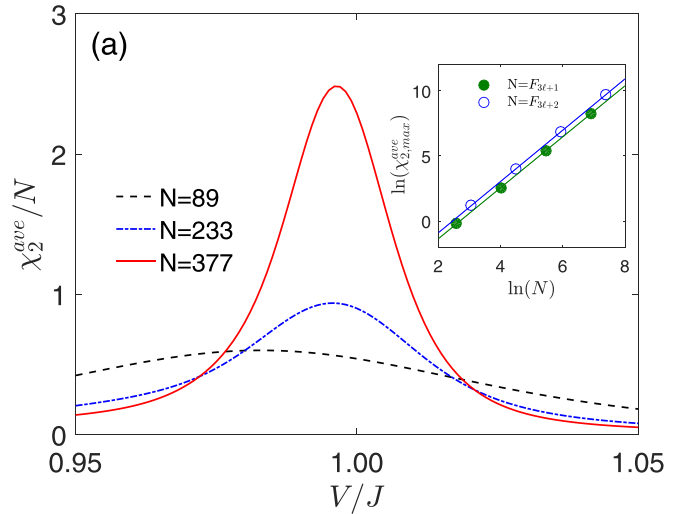


FIG. 8. The spectrum averaged fidelity susceptibility per site (a) χ_2^{ave}/N and (b) χ_2^{typ}/N as a function of the incommensurate potential strength V around $V_{c1} = 1.0$. The inset shows the scaling behavior of the maxima versus the system sizes for $N = F_{3\ell+1}$: 13, 55, 233, 987 and $N = F_{3\ell+2}$: 21, 89, 377, 1597. Here periodic boundary conditions are used with $\Delta = 0.5$, $\phi = 0$.

exponent agree well with each other. It is obvious that there is no qualitative difference between the spectrum-averaged fidelity susceptibilities (cf. Fig. 8) and the fidelity susceptibility of $|\psi_1\rangle$ [cf. Fig. 4(a)]. Therefore, it is sufficient to retrieve the universal information through the finite-size scaling of the lowest eigenstate for systems without mobility edges.

- [1] P. W. Anderson, Absence of diffusion in certain random lattices, *Phys. Rev.* **109**, 1492 (1958).
 [2] H. P. Lüschen, S. Scherg, T. Kohlert, M. Schreiber, P. Bordia, X. Li, S. Das Sarma, and I. Bloch, Single-Particle Mobility

- Edge in a One-Dimensional Quasiperiodic Optical Lattice, *Phys. Rev. Lett.* **120**, 160404 (2018).
 [3] H. Yao, A. Khoudli, L. Bresque, and L. Sanchez-Palencia, Critical Behavior and Fractality in Shallow One-Dimensional

- Quasiperiodic Potentials, *Phys. Rev. Lett.* **123**, 070405 (2019).
- [4] Y. Wang, X. Xia, L. Zhang, H. Yao, S. Chen, J. You, Q. Zhou, and X.-J. Liu, One-Dimensional Quasiperiodic Mosaic Lattice with Exact Mobility Edges, *Phys. Rev. Lett.* **125**, 196604 (2020).
- [5] J. Biddle, D. J. Priour, B. Wang, and S. Das Sarma, Localization in one-dimensional lattices with non-nearest-neighbor hopping: Generalized Anderson and Aubry-André models, *Phys. Rev. B* **83**, 075105 (2011).
- [6] J. Q. Liu and X. B. Bian, Multichannel High-Order Harmonic Generation from Fractal Bands in Fibonacci Quasicrystals, *Phys. Rev. Lett.* **127**, 213901 (2021).
- [7] D. Tanese, E. Gurevich, F. Baboux, T. Jacqmin, A. Lemaître, E. Galopin, I. Sagnes, A. Amo, J. Bloch, and E. Akkermans, Fractal Energy Spectrum of a Polariton Gas in a Fibonacci Quasiperiodic Potential, *Phys. Rev. Lett.* **112**, 146404 (2014).
- [8] N. Macé, N. Lafflorencie, and F. Alet, Many-body localization in a quasiperiodic Fibonacci chain, *SciPost Phys.* **6**, 050 (2019).
- [9] V. P. Michal, B. L. Altshuler, and G. V. Shlyapnikov, Delocalization of Weakly Interacting Bosons in a 1D Quasiperiodic Potential, *Phys. Rev. Lett.* **113**, 045304 (2014).
- [10] V. Mastropietro, Localization of Interacting Fermions in the Aubry-André Model, *Phys. Rev. Lett.* **115**, 180401 (2015).
- [11] M. Žnidarič and M. Ljubotina, Interaction instability of localization in quasiperiodic systems, *Proc. Natl. Acad. Sci. USA* **115**, 4595 (2018).
- [12] T. Kitagawa, E. Berg, M. Rudner, and E. Demler, Topological characterization of periodically driven quantum systems, *Phys. Rev. B* **82**, 235114 (2010).
- [13] M. Thakurathi, A. A. Patel, D. Sen, and A. Dutta, Floquet generation of Majorana end modes and topological invariants, *Phys. Rev. B* **88**, 155133 (2013).
- [14] L.-Z. Tang, S.-N. Liu, G.-Q. Zhang, and D.-W. Zhang, Topological Anderson insulators with different bulk states in quasiperiodic chains, *Phys. Rev. A* **105**, 063327 (2022).
- [15] H. Yao, T. Giamarchi, and L. Sanchez-Palencia, Lieb-Liniger Bosons in a Shallow Quasiperiodic Potential: Bose Glass Phase and Fractal Mott Lobes, *Phys. Rev. Lett.* **125**, 060401 (2020).
- [16] T. Bohlein and C. Bechinger, Experimental Observation of Directional Locking and Dynamical Ordering of Colloidal Monolayers Driven across Quasiperiodic Substrates, *Phys. Rev. Lett.* **109**, 058301 (2012).
- [17] S. Weidemann, M. Kremer, S. Longhi, and A. Szameit, Topological triple phase transition in non-Hermitian Floquet quasicrystals, *Nature (London)* **601**, 354 (2022).
- [18] L. Dal Negro, C. J. Oton, Z. Gaburro, L. Pavesi, P. Johnson, A. Lagendijk, R. Righini, M. Colocci, and D. S. Wiersma, Light Transport through the Band-Edge States of Fibonacci Quasicrystals, *Phys. Rev. Lett.* **90**, 055501 (2003).
- [19] Y. Lahini, R. Pugatch, F. Pozzi, M. Sorel, R. Morandotti, N. Davidson, and Y. Silberberg, Observation of a Localization Transition in Quasiperiodic Photonic Lattices, *Phys. Rev. Lett.* **103**, 013901 (2009).
- [20] W. DeGottardi, D. Sen, and S. Vishveshwara, Majorana Fermions in Superconducting 1D Systems Having Periodic, Quasiperiodic, and Disordered Potentials, *Phys. Rev. Lett.* **110**, 146404 (2013).
- [21] G. Modugno, Anderson localization in Bose-Einstein condensates, *Rep. Prog. Phys.* **73**, 102401 (2010).
- [22] G. Roati, C. D'Errico, L. Fallani, M. Fattori, C. Fort, M. Zaccanti, G. Modugno, M. Modugno, and M. Inguscio, Anderson localization of a non-interacting Bose-Einstein condensate, *Nature (London)* **453**, 895 (2008).
- [23] M. Schreiber, S. S. Hodgman, P. Bordia, H. P. Lüschen, M. H. Fischer, R. Vosk, E. Altman, U. Schneider, and I. Bloch, Observation of many-body localization of interacting fermions in a quasirandom optical lattice, *Science* **349**, 842 (2015).
- [24] P. Bordia, H. Lüschen, U. Schneider, M. Knap, and I. Bloch, Periodically driving a many-body localized quantum system, *Nat. Phys.* **13**, 460 (2017).
- [25] M. de Dios-Leyva, A. L. Morales, and C. A. Duque, Magnetoconductivity in quasiperiodic graphene superlattices, *Sci. Rep.* **10**, 21284 (2020).
- [26] T. Pertsch, U. Peschel, J. Kobelke, K. Schuster, H. Bartelt, S. Nolte, A. Tünnermann, and F. Lederer, Nonlinearity and Disorder in Fiber Arrays, *Phys. Rev. Lett.* **93**, 053901 (2004).
- [27] U. Agrawal, S. Gopalakrishnan, and R. Vasseur, Universality and quantum criticality in quasiperiodic spin chains, *Nat. Commun.* **11**, 2225 (2020).
- [28] U. Agrawal, S. Gopalakrishnan, and R. Vasseur, Quantum Criticality in the 2D Quasiperiodic Potts Model, *Phys. Rev. Lett.* **125**, 265702 (2020).
- [29] A. Chandran and C. R. Laumann, Localization and Symmetry Breaking in the Quantum Quasiperiodic Ising Glass, *Phys. Rev. X* **7**, 031061 (2017).
- [30] P. J. D. Crowley, A. Chandran, and C. R. Laumann, Quasiperiodic Quantum Ising Transitions in 1D, *Phys. Rev. Lett.* **120**, 175702 (2018).
- [31] V. Khemani, D. N. Sheng, and D. A. Huse, Two Universality Classes for the Many-Body Localization Transition, *Phys. Rev. Lett.* **119**, 075702 (2017).
- [32] A. Szabó and U. Schneider, Non-power-law universality in one-dimensional quasicrystals, *Phys. Rev. B* **98**, 134201 (2018).
- [33] K. Hida, New Universality Class in Spin-One-Half Fibonacci Heisenberg Chains, *Phys. Rev. Lett.* **93**, 037205 (2004).
- [34] V. Goblot, A. Štrkalj, N. Pernet, J. L. Lado, C. Dorow, A. Lemaître, L. Le Gratiet, A. Harouri, I. Sagnes, S. Ravets, A. Amo, J. Bloch, and O. Zilberberg, Emergence of criticality through a cascade of delocalization transitions in quasiperiodic chains, *Nat. Phys.* **16**, 832 (2020).
- [35] P. G. Harper, The general motion of conduction electrons in a uniform magnetic field, with application to the diamagnetism of metals, *Proc. Phys. Soc. A* **68**, 879 (1955).
- [36] M. Kohmoto, L. P. Kadanoff, and C. Tang, Localization Problem in One Dimension: Mapping and Escape, *Phys. Rev. Lett.* **50**, 1870 (1983).
- [37] H. Hiramoto and M. Kohmoto, Scaling analysis of quasiperiodic systems: Generalized Harper model, *Phys. Rev. B* **40**, 8225 (1989).
- [38] D. R. Hofstadter, Energy levels and wave functions of Bloch electrons in rational and irrational magnetic fields, *Phys. Rev. B* **14**, 2239 (1976).
- [39] B. B. Wei, Fidelity susceptibility in one-dimensional disordered lattice models, *Phys. Rev. A* **99**, 042117 (2019).
- [40] A. Sinha, M. M. Rams, and J. Dziarmaga, Kibble-Zurek mechanism with a single particle: Dynamics of the

- localization-delocalization transition in the Aubry-André model, *Phys. Rev. B* **99**, 094203 (2019).
- [41] S. Aubry and G. André, Analyticity breaking and Anderson localization in incommensurate lattices, *Ann. Israel Phys. Soc.* **3**, 133 (1980).
- [42] Q. B. Zeng, S. Chen, and R. Lü, Generalized Aubry-André-Harper model with p -wave superconducting pairing, *Phys. Rev. B* **94**, 125408 (2016).
- [43] X. Cai, L. J. Lang, S. Chen, and Y. Wang, Topological Superconductor to Anderson Localization Transition in One-Dimensional Incommensurate Lattices, *Phys. Rev. Lett.* **110**, 176403 (2013).
- [44] Y. Wang, Y. Wang, and S. Chen, Spectral statistics, finite-size scaling and multifractal analysis of quasiperiodic chain with p -wave pairing, *Eur. Phys. J. B* **89**, 254 (2016).
- [45] Y. Wang, H. Hu, and S. Chen, Many-body ground state localization and coexistence of localized and extended states in an interacting quasiperiodic system, *Eur. Phys. J. B* **89**, 77 (2016).
- [46] J. Wang, X.-J. Liu, G. Xianlong, and H. Hu, Phase diagram of a non-Abelian Aubry-André-Harper model with p -wave superfluidity, *Phys. Rev. B* **93**, 104504 (2016).
- [47] X. Tong, Y.-M. Meng, X. Jiang, C. Lee, G. D. d. M. Neto, and G. Xianlong, Dynamics of a quantum phase transition in the Aubry-André-Harper model with p -wave superconductivity, *Phys. Rev. B* **103**, 104202 (2021).
- [48] I. I. Satija, Symmetry breaking and stabilization of critical phase, *Phys. Rev. B* **48**, 3511 (1993).
- [49] T. Geisel, R. Ketzmerick, and G. Petschel, New Class of Level Statistics in Quantum Systems with Unbounded Diffusion, *Phys. Rev. Lett.* **66**, 1651 (1991).
- [50] K. Machida and M. Fujita, Quantum energy spectra and one-dimensional quasiperiodic systems, *Phys. Rev. B* **34**, 7367 (1986).
- [51] C. L. Bertrand and A. M. García-García, Anomalous Thouless energy and critical statistics on the metallic side of the many-body localization transition, *Phys. Rev. B* **94**, 144201 (2016).
- [52] A. D. Mirlin, Y. V. Fyodorov, A. Mildenerger, and F. Evers, Exact Relations between Multifractal Exponents at the Anderson Transition, *Phys. Rev. Lett.* **97**, 046803 (2006).
- [53] R. Dubertrand, I. García-Mata, B. Georgeot, O. Giraud, G. Lemarié, and J. Martin, Two Scenarios for Quantum Multifractality Breakdown, *Phys. Rev. Lett.* **112**, 234101 (2014).
- [54] S. Katsura, Statistical mechanics of the anisotropic linear Heisenberg model, *Phys. Rev.* **127**, 1508 (1962).
- [55] I. I. Satija and M. M. Doria, Localization and long-range order in magnetic chains, *Phys. Rev. B* **39**, 9757 (1989).
- [56] M. M. Doria and I. I. Satija, Quasiperiodicity and Long-Range Order in a Magnetic System, *Phys. Rev. Lett.* **60**, 444 (1988).
- [57] I. I. Satija, Spectral and magnetic interplay in quantum spin chains: Stabilization of the critical phase due to long-range order, *Phys. Rev. B* **49**, 3391 (1994).
- [58] Y. Wang, L. Zhang, S. Niu, D. Yu, and X.-J. Liu, Realization and Detection of Nonergodic Critical Phases in an Optical Raman Lattice, *Phys. Rev. Lett.* **125**, 073204 (2020).
- [59] T. Lv, T.-C. Yi, L. Li, G. Sun, and W.-L. You, Quantum criticality and universality in the p -wave-paired Aubry-André-Harper model, *Phys. Rev. A* **105**, 013315 (2022).
- [60] X. Zhang and S. F. Matthew, Enhanced Amplitude for Superconductivity due to Spectrum-wide Wave Function Criticality in Quasiperiodic and Power-law Random Hopping Models, [arXiv:2204.02996](https://arxiv.org/abs/2204.02996).
- [61] T. Liu, P. Wang, S. Chen, and X. Gao, Phase diagram of a generalized off-diagonal Aubry-André model with p -wave pairing, *J. Phys. B: At. Mol. Opt. Phys.* **51**, 025301 (2018).
- [62] D. S. Fisher, Critical behavior of random transverse-field Ising spin chains, *Phys. Rev. B* **51**, 6411 (1995).
- [63] A. B. Harris, Effect of random defects on the critical behaviour of Ising models, *J. Phys. C: Solid State Phys.* **7**, 1671 (1974).
- [64] K. Ino and M. Kohmoto, Critical properties of Harper's equation on a triangular lattice, *Phys. Rev. B* **73**, 205111 (2006).
- [65] L. Y. Gong and P. Q. Tong, Fidelity, fidelity susceptibility, and von Neumann entropy to characterize the phase diagram of an extended Harper model, *Phys. Rev. B* **78**, 115114 (2008).
- [66] T. Cookmeyer, J. Motruk, and J. E. Moore, Critical properties of the ground-state localization-delocalization transition in the many-particle Aubry-André model, *Phys. Rev. B* **101**, 174203 (2020).
- [67] M. E. Fisher and M. N. Barber, Scaling Theory for Finite-Size Effects in the Critical Region, *Phys. Rev. Lett.* **28**, 1516 (1972).
- [68] G. De Chiara, L. Lepori, M. Lewenstein, and A. Sanpera, Entanglement Spectrum, Critical Exponents, and Order Parameters in Quantum Spin Chains, *Phys. Rev. Lett.* **109**, 237208 (2012).
- [69] S. Ryu and T. Takayanagi, Holographic Derivation of Entanglement Entropy from the anti-de Sitter Space/Conformal Field Theory Correspondence, *Phys. Rev. Lett.* **96**, 181602 (2006).
- [70] N. S. Mazhari, D. Momeni, S. Bahamonde, M. Faizal, and R. Myrzakulov, Holographic complexity and fidelity susceptibility as holographic information dual to different volumes in AdS, *Phys. Lett. B* **766**, 94 (2017).
- [71] A. Osterloh, L. Amico, G. Falci, and R. Fazio, Scaling of entanglement close to a quantum phase transition, *Nature (London)* **416**, 608 (2002).
- [72] G. Vidal, J. I. Latorre, E. Rico, and A. Kitaev, Entanglement in Quantum Critical Phenomena, *Phys. Rev. Lett.* **90**, 227902 (2003).
- [73] S. J. Gu, S. S. Deng, Y. Q. Li, and H. Q. Lin, Entanglement and Quantum Phase Transition in the Extended Hubbard Model, *Phys. Rev. Lett.* **93**, 086402 (2004).
- [74] A. Hamma, R. Ionicioiu, and P. Zanardi, Bipartite entanglement and entropic boundary law in lattice spin systems, *Phys. Rev. A* **71**, 022315 (2005).
- [75] A. Kitaev and J. Preskill, Topological Entanglement Entropy, *Phys. Rev. Lett.* **96**, 110404 (2006).
- [76] Y. Zhang, T. Grover, and A. Vishwanath, Entanglement Entropy of Critical Spin Liquids, *Phys. Rev. Lett.* **107**, 067202 (2011).
- [77] M. Levin and X. G. Wen, Detecting Topological Order in a Ground State Wave Function, *Phys. Rev. Lett.* **96**, 110405 (2006).
- [78] I. Mondragon-Shem and T. L. Hughes, Signatures of metal-insulator and topological phase transitions in the entanglement of one-dimensional disordered fermions, *Phys. Rev. B* **90**, 104204 (2014).
- [79] N. Roy and A. Sharma, Study of counterintuitive transport properties in the Aubry-André-Harper model via entanglement

- entropy and persistent current, *Phys. Rev. B* **100**, 195143 (2019).
- [80] L. Y. Gong and P. Q. Tong, Von Neumann entropy of an electron in one-dimensional determined potentials, *Chin. Phys. Lett.* **22**, 2759 (2005).
- [81] L. Y. Gong and P. Q. Tong, Localization-delocalization transitions in a two-dimensional quantum percolation model: Von Neumann entropy studies, *Phys. Rev. B* **80**, 174205 (2009).
- [82] L. Y. Gong and P. Q. Tong, von Neumann entropy and localization properties of two interacting particles in one-dimensional nonuniform systems, *Phys. Rev. B* **76**, 085121 (2007).
- [83] G. Roósz, U. Divakaran, H. Rieger, and F. Iglói, Nonequilibrium quantum relaxation across a localization-delocalization transition, *Phys. Rev. B* **90**, 184202 (2014).
- [84] G. De Tomasi and I. M. Khaymovich, Multifractality Meets Entanglement: Relation for Nonergodic Extended States, *Phys. Rev. Lett.* **124**, 200602 (2020).
- [85] S. N. Evangelou and J.-L. Pichard, Critical Quantum Chaos and the One-Dimensional Harper Model, *Phys. Rev. Lett.* **84**, 1643 (2000).
- [86] A. Montakhab and A. Asadian, Multipartite entanglement and quantum phase transitions in the one-, two-, and three-dimensional transverse-field Ising model, *Phys. Rev. A* **82**, 062313 (2010).
- [87] R. Radgohar and A. Montakhab, Global entanglement and quantum phase transitions in the transverse XY Heisenberg chain, *Phys. Rev. B* **97**, 024434 (2018).
- [88] A. P. Siebesma and L. Pietronero, Multifractal properties of wave functions for one-dimensional systems with an incommensurate potential, *Europhys. Lett.* **4**, 597 (1987).
- [89] G. Roósz, Z. Zimborás, and R. Juhász, Entanglement scaling in fermion chains with a localization-delocalization transition and inhomogeneous modulations, *Phys. Rev. B* **102**, 064204 (2020).
- [90] B. Widom, Equation of state in the neighborhood of the critical point, *J. Chem. Phys.* **43**, 3898 (1965).
- [91] W. L. You, Y. W. Li, and S. J. Gu, Fidelity, dynamic structure factor, and susceptibility in critical phenomena, *Phys. Rev. E* **76**, 022101 (2007).
- [92] W. L. You and L. He, Generalized fidelity susceptibility at phase transitions, *J. Phys.: Condens. Matter* **27**, 205601 (2015).
- [93] S. J. Gu, Fidelity approach to quantum phase transitions, *Int. J. Mod. Phys. B* **24**, 4371 (2010).
- [94] A. F. Albuquerque, F. Alet, C. Sire, and S. Capponi, Quantum critical scaling of fidelity susceptibility, *Phys. Rev. B* **81**, 064418 (2010).
- [95] N. Chepiga and F. Mila, Kibble-Zurek exponent and chiral transition of the period-4 phase of Rydberg chains, *Nat. Commun.* **12**, 414 (2021).
- [96] P. Zanardi, M. Cozzini, and P. Giorda, Ground state fidelity and quantum phase transitions in free Fermi systems, *J. Stat. Mech.* (2007) L02002..
- [97] N. T. Jacobson, S. Garnerone, S. Haas, and P. Zanardi, Scaling of the fidelity susceptibility in a disordered quantum spin chain, *Phys. Rev. B* **79**, 184427 (2009).
- [98] S. Garnerone, N. T. Jacobson, S. Haas, and P. Zanardi, Fidelity Approach to the Disordered Quantum XY Model, *Phys. Rev. Lett.* **102**, 057205 (2009).
- [99] I. Peschel, Calculation of reduced density matrices from correlation functions, *J. Phys. A: Math. Theor* **36**, L205 (2003).
- [100] M. Cozzini, P. Giorda, and P. Zanardi, Quantum phase transitions and quantum fidelity in free fermion graphs, *Phys. Rev. B* **75**, 014439 (2007).